WATER RESOURCES RESEARCH, VOL. 31, NO. 4, PAGES 961–968, APRIL 1995

Watershed scale shear stress from tethersonde wind profile measurements under near neutral and unstable atmospheric stability

M. B. Parlange[1] and G. G. Katul
Hydrologic Science, University of California, Davis

Abstract. Mean wind speed profiles were measured in the atmospheric surface layer, using a tethersonde system, above the Ojai Valley Watershed in southern California. The valley is mainly planted with mature avocado and orange trees. The surface shear stress and latent and sensible heat fluxes were measured above the trees which are up to 9 m in height. Near-neutral wind speed profile measurements allowed the determination of the watershed surface roughness (z_0 = 1.4 m) and the momentum displacement height (d_0 = 7.0 m). The wind speed measurements obtained under unstable atmospheric stability were analyzed using Monin-Obukhov similarity theory. New stability correction functions proposed based on theory and experiments of Kader-Yaglom as well as the now classic Businger-Dyer type functions were tested. The watershed shear stress values calculated using the surface layer wind speed profiles with the new Monin-Obukhov stability functions were found to be improved in comparison with the values obtained with the Businger-Dyer functions under strongly unstable stability conditions. The Monin-Obukhov model with the Businger-Dyer stability correction function underpredicted the momentum flux by 25% under strongly unstable stability conditions, while the new Kader-Yaglom formulation compared well on average (R^2 = 0.77) with the surface eddy correlation measurements for all atmospheric stability conditions. The unstable 100-m drag coefficient was found to be u_*^2/V_{100}^2 = 0.0182.

1. Introduction

Analysis of surface layer profile measurements of wind speed, temperature, and specific humidity in the atmospheric boundary layer (ABL) in the context of Monin-Obukhov similarity theory has shown great promise for the determination of regional scale heat and momentum surface fluxes [e.g., *Brutsaert*, 1986; *Brutsaert and Kustas*, 1987; *Brutsaert and Sugita*, 1990; *Brutsaert and Parlange*, 1992; *Parlange and Brutsaert*, 1993]. For the estimation of sensible heat or latent heat fluxes into the atmosphere it is necessary to know the friction velocity u_* [$= (\tau_0/\rho)^{1/2}$], where τ_0 is the surface shear stress and ρ is the density of the air. The friction velocity given in terms of *Monin and Obukhov* [1954] similarity theory based on the wind speed gradient is

$$\frac{dV}{dz} = \frac{u_*}{k(z - d_0)}\,\phi_m(y) \tag{1}$$

where V is the mean wind speed, k is von Kármán's constant (= 0.4), and z is the height above the ground. The Monin-Obukhov stability function $\phi_m = \phi_m(y)$ is a function of the dimensionless parameter $[(z - d_0)/L]$, where L is the Obukhov length:

$$L = \frac{-u_*^3}{kg[H_v/\rho c_p T_a]} \tag{2}$$

$H_v = (H + 0.61 T_a C_p E)$ is the specific flux of virtual sensible heat, H is the specific flux of sensible heat, E is the evaporation rate, g is the acceleration of gravity, c_p is the specific heat at constant pressure, and T_a is the air temperature. Most experimental studies to determine the stability function ϕ_m have been carried out at local field scales, where atmospheric profile measurements are rarely measured beyond a height of 10 m. As a result, the behavior of ϕ_m for large $-y$ (> 3.0), in general, has not been studied as extensively [*Holtslag*, 1984; *Kader and Yaglom*, 1990; *Parlange and Brutsaert*, 1993]. Based on the local field studies, the classic Businger-Dyer formulation [e.g., *Dyer*, 1974; *Hicks*, 1976; *Businger*, 1988; *Hogstrom*, 1988] of the stability correction function,

$$\phi_m = (1 - Cy)^{-1/4} \tag{3}$$

where C is a constant, is routinely used in field scale applications of Monin-Obukhov similarity theory [e.g., *Parlange and Katul*, 1992a, b; *Katul and Parlange*, 1992a, b]. However, for regional scale flux studies where the profile measurements are made relatively high above the land surface [*Brutsaert et al.*, 1989] or for strongly unstable conditions, implying small L, the Businger-Dyer formulation might not perform as well as for local scale studies. *Holtslag* [1984] noted that the Businger-Dyer form may be valid for $-y < 7$; however, in regional land-atmosphere studies values of $-y$ up to 15 may be important in practice, and there is a need for further investigation.

[1]Also at Department of Biological and Agricultural Engineering, University of California, Davis.

Paper number 94WR01949.
0043-1397/95/94WR-01949$05.00

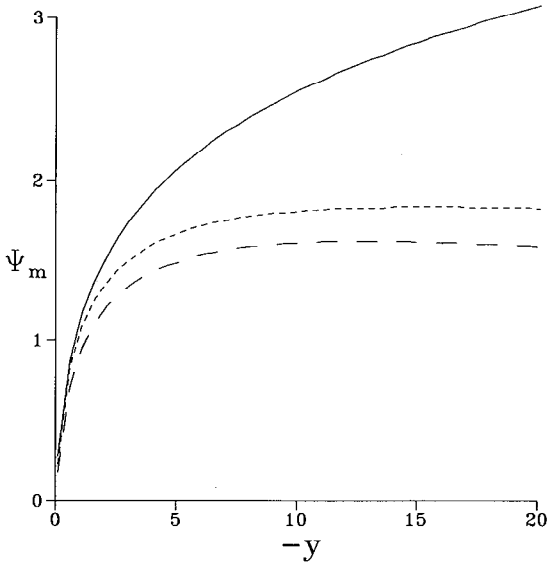

Figure 1. The integrated momentum stability correction function Ψ_m ($z_0 = 0$): solid line, equation (7); long-dashed line, equation (8); short-dashed line, equation (9).

Kader and Yaglom [1990] recently reported, on the basis of an extensive set of measurements, values of ϕ_m for $-y$ up to 20 (due to small L). Their work extended results of directional dimensional analysis due to *Zilitinkevich* [1971] and *Betchov and Yaglom* [1971] to develop a new ϕ_m equation. Using the results of *Kader and Yaglom* [1990], *Brutsaert* [1992] presented an interpolation formula:

$$\phi_m = [(a + bx^n)/(a + x^n)] + cx^{1/3} \tag{4}$$

where $x = -y$, and a, b, c, and n are constants which may be selected to match the Kader-Yaglom ϕ_m. Brutsaert suggested the use of (4), since in most surface flux calculations the integral of (1),

$$V = \frac{u_*}{k}\left[\ln\left(\frac{z - d_0}{z_0}\right) - \psi_m(y)\right] \tag{5}$$

is usually applied, where z_0 is the surface roughness length and

$$\psi_m(y) = \int_{z_0/L}^{y} [1 - \phi(z)]\, dz/z \tag{6}$$

which is not easily solved analytically using the original *Kader and Yaglom* [1990] ϕ_m equation. Integrating (1) with (3) and (4) gives [*Paulson*, 1970]

$$\psi_m(y) = \ln\left[\frac{(1 + u)^2(1 + u^2)}{(1 + u_0)^2(1 + u_0^2)}\right] - 2\arctan(u) + 2\arctan(u_0) \tag{7}$$

and [*Brutsaert*, 1992]

$$\psi_m(y) = 0 \qquad y > -0.0093 \tag{8a}$$

$$\psi_m(y) = 1.72\ln\left[\frac{(0.37 + x^{0.72})}{0.37 + (0.0093 + x_0)^{0.72}}\right] - 1.50[x^{1/3} - (0.0093 + x_0)^{1/3}] \qquad y \le -0.0093 \tag{8b}$$

respectively, where $u = (1 - 16y)^{1/4}$, $u_0 = (1 - 16z_0/L)^{1/4}$, $x_0 = -z_0/L$, and the appropriate constants have been inserted in (8). *Brutsaert* [1992] also made a proposal as to the selection of the constants in (4), or (8), to allow a closer fit to (2) for small x and remain more constant for large x:

$$\psi_m(y) = 0 \qquad y > -0.0059 \tag{9a}$$

$$\psi_m(y) = 1.47\ln\left[\frac{(0.28 + x^{0.75})}{0.28 + (0.0059 + x_0)^{0.75}}\right] - 1.29[x^{1/3} - (0.0059 + x_0)^{1/3}] \qquad -0.0059 \le y \le -15.025 \tag{9b}$$

$$\psi_m(y) = \psi_m(-15.025) \qquad y \le -15.025 \tag{9c}$$

This suggestion is appropriate; it is important to incorporate the Businger-Dyer results, since so many field experiments have gone into the testing and validation of (2) [*Hogstrom*, 1988; *Brutsaert*, 1992]. The three Ψ_m functions (7), (8), and (9) for $z_0 = 0$ are plotted in Figure 1. *Parlange and Brutsaert* [1993] carried out an analysis of wind speed profiles measured with radiosondes under unstable atmospheric conditions over the Landes Forest in southwestern France, as part of the HAPEX-MOBILHY field campaign [*André et al.*, 1986, 1988]. The radiosonde wind profiles were studied using the Monin-Obukhov mean wind speed profile equation (5) with each of (7), (8), and (9) to explore the usefulness of the model in calculating the regional u_*. The u_* values derived from the Monin-Obukhov model wind speed profile with Ψ_m given by (9) agreed slightly better with eddy correlation measurements [*Gash et al.*, 1989; *Shuttleworth et al.*, 1988] than with Ψ_m given by (7) or (8), although the results were not entirely conclusive. It is crucial then that for the calculation of regional evaporation, other studies examine the Monin-Obukhov stability correction functions for large $-(z - d_0)/L$. In this study, values of $-y$ up to 15 were measured.

The behavior of Ψ_m for large values of $-y$ is an important issue in regional evaporation studies because the lower limit where similarity theory can be applied is usually well above the land surface. *Thom et al.* [1975] were the first to point out the breakdown of surface layer similarity near the top of forests. *Garratt* [1978, 1979, 1980] and many other researchers [e.g., *Raupach*, 1979; *Raupach and Thom*, 1981; *Denmead and Bradley*, 1985; *Cellier*, 1986; *Chen and Schwerdtfeger*, 1989; *Brutsaert et al.*, 1989; *Parlange and Brutsaert*, 1990, 1993; *Brutsaert and Parlange*, 1992] have shown that the regional transition layer height where it is appropriate to use surface layer similarity to describe wind speed measurements, or any scalar profile, is some 30–$60z_0$. This lower limit (i.e., $30z_0$) may be overly restrictive, but the vertical resolution of most wind speed profilers does not allow for closer detail.

In this paper, wind speed profiles measured with a tethersonde system at the upwind end of the Ojai Valley watershed in southern California under near neutral and unstable atmospheric conditions are analyzed. The primary focus of this study is to investigate the usefulness of Monin-Obukhov similarity theory with the different stability correction functions to estimate the regional scale friction velocity u_* under

different levels of unstable atmospheric stability. In particular, the relative merits of (7), (8), and (9) are studied on the basis of comparisons with eddy correlation surface flux measurements. The watershed surface roughness parameters z_0 and d_0 are first obtained from wind profiles measured under neutral atmospheric stability. Then the wind profiles measured under unstable stability conditions for $-y < 3$ are analyzed to check that analyzing the tethersonde wind profile measurements with Businger-Dyer correction functions in the context of Monin-Obukhov similarity is indeed satisfactory. This first analysis represents a type of error analysis which provides us with confidence to explore further the behavior of the stability correction function for $-y > 3$. Finally, the 100-m unstable drag coefficient is determined to provide a quick way to obtain useful friction velocity estimates.

2. Experiment

The tethersonde wind speed profiles were measured during July 1990 over the Ojai Valley in southern California (see Table 1). The profile sounding point was located at the easternmost end of the valley so as to maximize the upwind fetch, since the prevailing winds are westerly. The watershed extends some 12 km west to east and about 2–3 km north to south. The terrain is flat with the exception of the surrounding hills which are about 50–300 m and enclose the watershed to the north, south, and east. To the west beyond the valley the terrain consists of smaller hills interspersed with avocado and citrus groves. The Ojai Valley itself is almost entirely covered with densely grown avocado trees averaging roughly 7 m in height. The trees extend part way up the sides of the hills and are microsprinkler irrigated throughout, so that water is not a limiting factor for the trees.

The ABL surface layer profile measurements were obtained using an AIR TS-1A-1 tethersonde, situated in a clearing, which measured dry bulb and wet bulb depression, wind speed, and wind direction. The wind speed is measured with a 3-cup anemometer, and the wind direction is measured by a magnetic compass. The cup anemometer is accurate to ± 0.25 m s^{-1} for a wind speed range of 0.5–20 m s^{-1}. The instrument package was raised and lowered with a tethered 3.25-m^3 blimp attached to a battery-powered winch. Profile measurements were made every 10 m up to 100 m and then every 20 m up to 200 m. Only those profiles in which the tethersonde maintained near-vertical and smooth ascent or descent were used in the analysis. At each measurement elevation three readings of each of the atmospheric parameters were recorded and averaged over a 1- to 2-min period.

The surface momentum and heat fluxes were measured using an eddy correlation system situated 50 m from the tethersonde profiling winch. Most of the eddy correlation instruments were mounted at 13 m over a 7-m-tall avocado grove. The atmospheric water vapor was measured with a fast response infrared gas analyzer unit (model E009, Advanced System Inc.). The fluctuations in vertical velocity and temperature were measured simultaneously with a one-dimensional vertical sonic anemometer and a 13-μm type E thermocouple, respectively (model CA27, Campbell Scientific). The friction velocity u_* was obtained from a triaxial sonic anemometer set at 12 m (model BH-478B/3, Applied Technology). All the fast response data were collected at 10 Hz and stored on a personal computer. By using the fast response measurements the average turbulent fluxes were obtained for 30-min time periods. It is reasonable to assume that the eddy correlation flux measurements are representative of the watershed scale surface fluxes given the homogeneity of the valley. A total of 29 surface layer profile measurements were made when the eddy correlation flux system was fully functional. These profiles are used in the analysis below.

Table 1. Profiles and the Corresponding Eddy Correlation 30-min Average Friction Velocities u_* and Latent (LE), and Sensible Heat (H) Fluxes

Profile	Year Day	Time, PDT	u_*, m s^{-1}	LE, W m^{-2}	H, W m^{-2}	$-L$, m
1	200	1635	0.36	116	47	99.46
2	202	0902	0.18	256	8	77.94
3	202	1020	0.40	396	116	53.29
4	202	1054	0.56	325	246	71.00
5	202	1535	0.57	256	134	135.18
6	202	1602	0.55	233	114	147.68
7	202	1650	0.49	116	18	656.91
8	203	0919	0.31	104	140	20.62
9	203	0934	0.31	349	106	27.23
10	203	1012	0.24	302	106	12.81
11	203	1032	0.23	349	140	8.13
12	203	1310	0.63	372	261	94.52
13	203	1507	0.72	418	278	131.92
14	204	0900	0.22	209	77	13.48
15	204	0945	0.21	256	121	7.80
16	204	1030	0.35	325	172	24.43
17	204	1110	0.26	325	182	9.55
18	204	1153	0.41	289	297	23.04
19	204	1358	0.75	348	271	151.39
20	204	1445	0.71	325	250	138.47
21	204	1652	0.69	256	150	217.60
22	204	1734	0.57	186	106	177.14
23	204	1750	0.54	162	73	213.96
24	204	1812	0.51	116	47	284.36
25	205	0952	0.30	280	120	22.49
26	205	1103	0.27	302	165	12.29
27	205	1130	0.27	349	175	11.59
28	205	1302	0.67	349	292	102.11
29	205	1715	0.63	256	161	153.22

Here, PDT is Pacific daylight time.

3. ABL Surface Layer Wind Speed Analysis

3.1. Near-Neutral Wind Speed Analysis

To apply (5), it is necessary to know the watershed roughness length and momentum displacement height. *Parlange and Brutsaert* [1989, 1990, 1993] found that once z_0 and d_0 had been established, even somewhat erratic wind profiles could be used to obtain reliable u_*. This is important, since the ability to obtain realistic watershed evaporation with surface layer similarity is directly linked to the accuracy with which u_* is estimated.

To obtain the regional momentum surface parameters we used the procedure *Kustas and Brutsaert* [1986], *Parlange and Brutsaert* [1989, 1990], and *Sugita and Brutsaert* [1990] have successfully applied to near-neutral wind profile measurements. If wind profile measurements are made when the surface heat fluxes are small and the momentum flux is large (e.g., $|L| > 160$ m) and not during a stability transition period, the logarithmic wind profile

Table 2. Near-Neutral Profile Analysis Results; z_{0m}, Profile-Derived u_{*n}, and Surface Layer Range

Profile	$-L$, m (Eddy Correction)	z_{0m}, m	u_{*n}, m/s	Range
7	657	1.18	0.67	20–40
21	218	2.00	0.64	30–60
22	177	1.49	0.47	20–160
23	214	1.56	0.55	10–120
24	284	0.95	0.43	10–50

$$V = \frac{u_*}{k}\left[\ln\left(\frac{z-d_0}{z_0}\right)\right] \tag{10}$$

may be applied. Since we are interested in a permeable plant canopy, we rewrite the momentum displacement length as $d_0 = 5z_0$ [*Paeschke*, 1937; *Brutsaert*, 1982].

There were five wind profiles measured at times when the Obukhov length, calculated from the eddy correlation flux measurements, was greater than 160 m, which we classify as being near-neutral atmospheric stability. In particular, note the sequence of four wind speed profile measurements during the afternoon of year day 204 (see Table 1). Following *Parlange and Brutsaert* [1989], the z_0 and d_0 ($= 5z_0$) values were estimated by fitting (10) to the largest consecutive section of wind speed measurements, which produces a z_0 value within the range of 0.5–2.5 m. For tree canopies of height about 7–9 m, these limits are reasonable. It is known already from published surface roughnesses that the z_0 should be of the order of 1 m [see *Brutsaert*, 1982; *Panofsky and Dutton*, 1984; *Stull*, 1988; *Garratt*, 1978, 1980; *Parlange and Brutsaert*, 1990].

The results of the near-neutral wind speed profile analysis are presented in Table 2. An example of one of the wind profiles analyzed and the determination of z_0 is presented in Figure 2. The solid rectangles are those used in the analysis. The open rectangle closest to the land surface is in the roughness wake layer of the canopy, while the upper two rectangles extend beyond the surface layer. Note that the lower limit of the dynamic layer (Table 2) is found to be below the value of $30z_0$, which may be related to the increased vertical resolution of the sounding system. The average z_0 calculated was 1.4 m, and the corresponding d_0 was 7 m. These surface roughness parameters are used in the unstable analysis below to assess the performance of the stability correction functions. The examination of the stability correction function performance is independent of the surface roughness parameter calculation.

3.2. The ABL Surface Layer Range

As was discussed earlier, it is well known that atmospheric profile measurements above the roughness wake layer must be used for the application of (1) or (5). The lower limit of the surface layer, often called the transition or blending layer height, can often be taken as $50z_0$ [e.g., *Brutsaert and Parlange*, 1992]. The upper limit for the application of surface layer similarity for this watershed scale study can be considered fetch dependent, since beyond 12 k the terrain does not remain uniformly tree covered. A usual "rule of thumb" fetch to height ratio of 100 to 1 might be assumed, which would correspond to an upper surface layer height of 120 m. Although we have reasonable estimates of the height range for which the thersonde measurements may be applied, it is not entirely clear what range of upwind footprint area is reflected in profile measurements at a given height in the surface layer [e.g., *LeClerc and Thurtell*, 1990; *Schuepp et al.*, 1990]. As part of a preliminary analysis, we allowed all the wind profile measurements to be considered in establishing the optimal ranges of the surface layer for each of the individual wind speed profiles. Presumably, since we rely on the eddy correlation measurements obtained over the trees in the watershed, the upper limit found for the optimal surface layer ranges will directly reflect the watershed characteristics in this analysis.

The optimal height ranges for the application of (5) were established for each of (7), (8), and (9) by selecting the consecutive range of wind speed measurements for a given profile which gave a u_* value that numerically matched the closest the eddy correlation value. Since the same surface flux values are used for each stability correction function, each optimal boundary layer profile range is referenced to the same surface flux conditions. The disadvantage of using this approach, of course, is that the identification of the surface layer height range becomes dependent on the individual stability correction function. On the other hand, for actually testing the performance of each ψ it is useful to allow the "best" possible range for each individual function for comparison. A minimum set of three consecutive wind profile measurements was allowed to define the surface layer range for a given profile, and all the wind speed measurements from 20 to 200 m were considered in the analysis. The limits identified for each profile and stability function are presented in Table 3. The mean (± standard deviation) surface layer optimal ranges determined using all 29 profiles are

Equation (7)

$$71(\pm 39)\ \text{m} \le z \le 142(\pm 51)\ \text{m} \tag{11a}$$

Equation (8)

$$52(\pm 29)\ \text{m} \le z \le 110(\pm 49)\ \text{m} \tag{11b}$$

Equation (9)

$$59(\pm 39)\ \text{m} \le z \le 132(\pm 46)\ \text{m} \tag{11c}$$

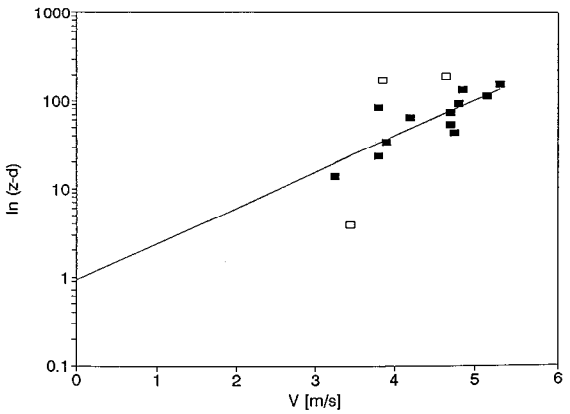

Figure 2. Profile of horizontal wind speed measured under near-neutral stability (profile 23). The straight line is the least squares regression through the solid rectangles.

Table 3. Optimal Friction Velocities Obtained Using Stability Functions (7), (8), and (9) for Each Individual Profile

		Equation (7)			Equation (8)			Equation (9)		
Profile	u_{*ec}, m/s	u_*, m/s	Min, m	Max, m	u_*, m/s	Min, m	Max, m	u_*, m/s	Min, m	Max, m
1	0.36	0.47	100	160	0.44	100	160	0.46	100	160
2	0.18	0.18	20	80	0.18	30	60	0.18	70	100
3	0.4	0.40	70	140	0.40	40	100	0.40	30	140
4	0.56	0.55	20	60	0.56	20	50	0.54	20	60
5	0.57	0.59	140	200	0.57	100	180	0.57	140	200
6	0.55	0.60	140	200	0.56	140	200	0.59	140	200
7	0.49	0.49	60	180	0.49	50	90	0.49	20	200
8	0.31	0.32	90	200	0.31	50	120	0.31	70	140
9	0.31	0.30	70	120	0.27	80	120	0.29	80	120
10	0.24	0.25	120	180	0.24	40	200	0.24	90	160
11	0.23	0.36	100	180	0.23	80	200	0.23	140	200
12	0.63	0.63	50	160	0.63	80	120	0.63	30	160
13	0.72	0.72	30	180	0.72	60	120	0.72	70	160
14	0.22	0.22	100	200	0.22	40	140	0.22	20	180
15	0.21	0.24	140	200	0.21	50	90	0.21	30	160
16	0.35	0.35	60	180	0.35	50	140	0.35	60	90
17	0.26	0.27	70	120	0.26	30	100	0.26	30	140
18	0.41	0.41	60	160	0.38	80	120	0.41	80	120
19	0.75	0.59	80	140	0.56	40	90	0.58	40	90
20	0.71	0.72	30	80	0.71	20	50	0.71	30	80
21	0.69	0.66	30	60	0.63	30	60	0.65	30	60
22	0.57	0.57	100	160	0.57	50	80	0.57	30	160
23	0.54	0.54	20	100	0.54	20	80	0.54	20	100
24	0.51	0.50	20	60	0.52	20	50	0.50	20	60
25	0.3	0.34	140	200	0.30	70	200	0.30	120	200
26	0.27	0.27	80	200	0.27	20	50	0.27	70	140
27	0.27	0.29	30	60	0.26	20	70	0.27	30	80
28	0.67	0.69	60	90	0.67	60	100	0.68	60	90
29	0.63	0.63	30	80	0.63	30	60	0.63	30	80
Mean			71.0	142.4		51.7	110.3		58.6	132.1
s.d.			39.4	51.2		29.1	48.7		38.5	46.1

Min, minimum height from surface; max, maximum height from surface; u_{*ec}, eddy correlation u_*.

Note that on average the lower limit of the surface layer is at least 50 m above the ground for each of the stability correction functions used with (5). This is in agreement with earlier findings on the applicability of Monin-Obukhov similarity over tree-covered regions [*Brutsaert and Parlange*, 1992]. The lower limit of the Businger-Dyer optimal range was somewhat higher than either (8) or (9), as was also noted by *Parlange and Brutsaert* [1993]. The lower limits on average were 20 m below those found in the Landes region. This could be attributed to the use of a tethersounding system which has a finer vertical resolution. In addition, since the Landes region is much more heterogeneous (broken) and surface fluxes from many different surfaces are being blended together, the atmosphere takes longer to integrate the different flux contributions. The upper limit scaling appears to be based on the upwind unbroken avocado and citrus fetch conditions (i.e., 12 km).

The question now is, How reliable is (5) with each of the different stability correction functions (7), (8), and (9) with the surface layer ranges specified above to obtain regional u_*? Furthermore, it is particularly interesting to explore how the stability correction functions effect the u_* calculated under strongly unstable atmospheric stability. An analysis is presented next of the wind profiles using the mean ranges given in (11) for each of the different stability correction functions.

3.3. Surface Layer Similarity Flux Determination

All the wind speed profiles were analyzed with the Monin-Obukhov mean wind speed profile model with Ψ_m given by (7), (8), and (9) to calculate u_*. The wind speed measurements with surface layer limits [70–140] m, [50–120] m, and [60–140] m (see Table 3) were used with (7), (8), and (9), respectively. In this way there is no bias toward one individual stability correction function.

The surface layer similarity analysis was carried out with linear regression of $\ln [(z - d_0)/\exp (\Psi_m(y))] - \ln (z_0)$ versus V, through the origin using for each profile the wind speed measurements for the mean ranges according to the stability correction function being tested. The Obukhov length used to determine Ψ_m was provided from the eddy correlation flux measurements so as not to bias any specific formulation. An overall regression analysis of the u_* profile derived values versus the three-dimensional sonic u_* for each of the stability correction functions is given in Tables 4 and 5. A comparison of the profile-derived friction velocities and those measured with the eddy correlation system is presented in Figures 3, 4, and 5 based on the stability correction functions (7), (8), and (9), respectively. There is no significant difference in the correlation coefficients at the 0.05 level of significance. The slopes of the regression lines forced through the origin are not significantly different from

Table 4. Regression Analysis of Friction Velocities From Monin-Obukhov Profile Analysis u_{*p} and Eddy Correlation u_{*ec} for (7), (8), and (9)

Stability Range	A	B	Coefficient of Determination, R^2	Standard Error of Estimate
		Equation (7)		
All y	0.97	−0.01	0.62	0.11
$-z_{ul}/L < 3$	0.72	0.18	0.55	0.10
$-z_{ul}/L > 3$	0.12	0.24	0.02	0.06
		Equation (8)		
All y	0.97	0.03	0.77	0.09
$-z_{ul}/L < 3$	0.76	0.16	0.56	0.10
$-z_{ul}/L > 3$	0.62	0.10	0.31	0.05
		Equation (9)		
All y	0.95	0.03	0.77	0.09
$-z_{ul}/L < 3$	0.73	0.17	0.57	0.10
$-z_{ul}/L > 3$	0.61	0.10	0.38	0.05

Values are based on wind speed measurements in the fixed height ranges 70–140 m, 50–120 m, and 60–140 m for (7), (8), and (9), respectively. The regression model is $u_* = Au_{*p} + B$. The regression results are presented for all the profiles analyzed (overall, $n = 29$) and for $-z_{ul}/L < 3$ ($n = 17$) and $-z_{ul}/L > 3$ ($n = 12$).

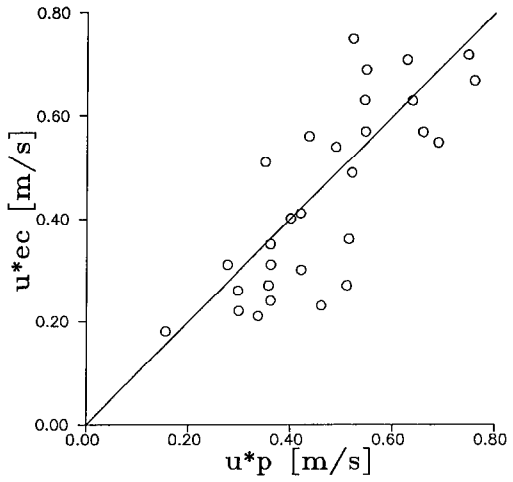

Figure 3. Comparison between the u_{*p} values derived from the wind profiles [70–140] m analyzed with Monin-Obukhov similarity with the Businger-Dyer stability correction function (7), and the eddy-correlation-measured u_{*ec} values. The coefficient of determination is $R^2 = 0.62$.

1.0 at the 95% confidence level, although using (7) gave a slope (0.95) which was furthest from 1.0.

It is instructive to split the profiles into two separate sets based upon the value of $-z_{ul}/L$, where z_{ul} is the upper height on the optimal surface layer range and L is calculated from the eddy flux measurements. The 29 soundings are split into those times when $-z_{ul}/L < 3$ or $-z_{ul}/L > 3$. The cutoff value of $-z/L = 3$ corresponds to the maximum value found in most available experimental data sets, which are primarily local scale. The analysis of the 17 profiles for which $-z_{ul}/L < 3$ represents a baseline analysis with which to compare the results using the other profiles, since the values fall into the range for which the Businger-Dyer results were based. For each of the stability correction functions there were 12 profiles measured when $-z_{ul}/L > 3$. The regression analysis is repeated for the second set (see Tables 4 and 5).

For $-z_{ul}/L < 3$ the slopes of the regression lines through the origin are not statistically different from 1.0 at the 95% confidence level. Equation (8) gave the forced regression slope (1.04) the furthest from 1.0, while both (7) and (9) gave the same forced regression slope of 1.02.

For $-z_{ul}/L > 3$ the slope of the forced regression line using (8) was found to be 0.95; using (9) it was 0.93. The slope of the forced regression using the Businger-Dyer (7) stability correction function was found to be 0.74. The strongly unstable subset is limited to only 12 profiles; nevertheless, this result supports the work of *Kader and Yaglom* [1990] in that the integrated stability correction function appears to be smaller for large $-(z - d_0)/L$ compared to (7). Apparently, (7) is less appropriate for large $-y$. This confirms the *Parlange and Brutsaert* [1993] analysis of the HAPEX-MOBILHY data set which indicated that the Businger-Dyer function should not necessarily be extended out past $-(z - d_0)/L$ equal to 3.

Table 5. Statistics of the Forced Regression Model $u_p^* = Au_{*ec}$

Profile Limits	Stability Range	Number of Observations	A	Standard Error of Estimate, m s^{-1}
		Equation (7)		
70–140 m	all y	29	0.95	0.11
	$-z_{ul}/L < 3$	17	1.02	0.11
	$-z_{ul}/L > 3$	12	0.74	0.07
		Equation (8)		
50–120 m	all y	29	1.02	0.09
	$-z_{ul}/L < 3$	17	1.04	0.11
	$-z_{ul}/L > 3$	12	0.95	0.05
		Equation (9)		
60–140 m	all y	29	1.01	0.09
	$-z_{ul}/L < 3$	17	1.02	0.11
	$-z_{ul}/L > 3$	12	0.93	0.05

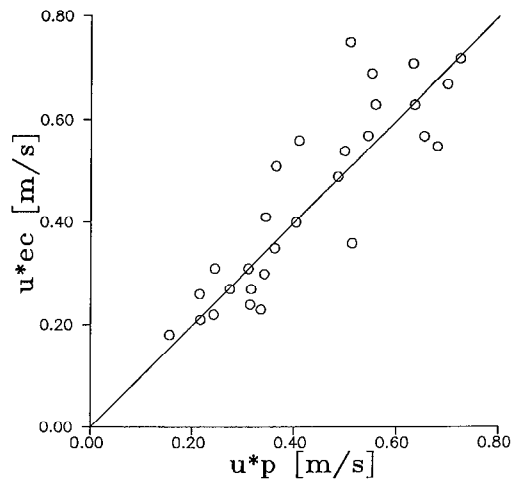

Figure 4. Same as Figure 3 but with the stability correction function (8) and wind profile range [50–120] m. The coefficient of determination is $R^2 = 0.77$.

3.4. Unstable Drag Coefficient (100 m)

For practical applications in both hydrologic and atmospheric science it is often helpful to estimate the shear stress with a drag coefficient:

$$Cd_r = u_*^2/V_r^2 \tag{12}$$

The reference height r used here is 100 m. Regression forced through the origin of V measured at 100 m for each profile versus the eddy correlation u_* gave a Cd_{100} of 0.0182. This is similar to the result obtained over the Landes region of 0.0173 [*Parlange and Brutsaert*, 1992]. The close match in the drag coefficients may be considered fortuitous; more experiments are needed at other sites to test these values. The u_* obtained with the drag coefficient are compared with the three-dimensional sonic measurements in Figure 6.

4. Conclusions

ABL surface layer similarity theory is a potentially powerful approach in regional hydrology to estimate surface fluxes over rough or complex land surfaces. Recently, there have been a number of issues raised concerning the formulation of the momentum stability correction function for the estimation of the surface shear stress. Some suggestions initiated due to the theory and analysis of *Kader and Yaglom* [1990] on the momentum stability correction function were tested in this study using tethersonde wind speed profiles measured over the Ojai Valley in southern California. The Monin-Obukhov similarity model with the Businger-Dyer stability correction function performed well for $-z_{ul}/L < 3$, which is in accordance with the extensive body of experimentation and analysis of (7). However, for strongly unstable conditions the value of the stability correction with Businger-Dyer appears to be too large. Based on the results found here, (8) and (9) appear to provide some improvement for the calculation of u_* based on comparisons with eddy correlation surface flux measurements. Although the results given here should be universally valid with regard to the similarity theory and future applications elsewhere, it is most important that further experiments be carried over other regions to test the reliability of both (8) and (9). It should be emphasized that the success of the Businger-Dyer stability correction functions for $-(z - d_0)/L$ is due in a large part to the extensive field testing and analysis that took place during the 1970s and 1980s. A similar effort needs to be made to establish the behavior of Ψ_m for regional studies. Finally, as a simple approach to estimate u_*, the 100-m drag coefficient over this watershed was $C_d = 0.0182$.

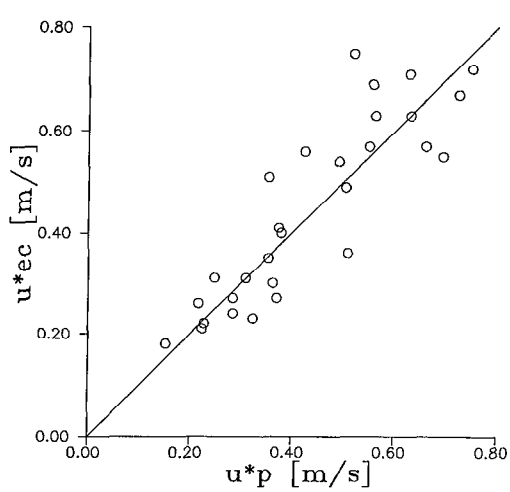

Figure 5. Same as Figure 3 but with the stability correction function (9) and the wind range [60–140] m. The coefficient of determination is $R^2 = 0.77$.

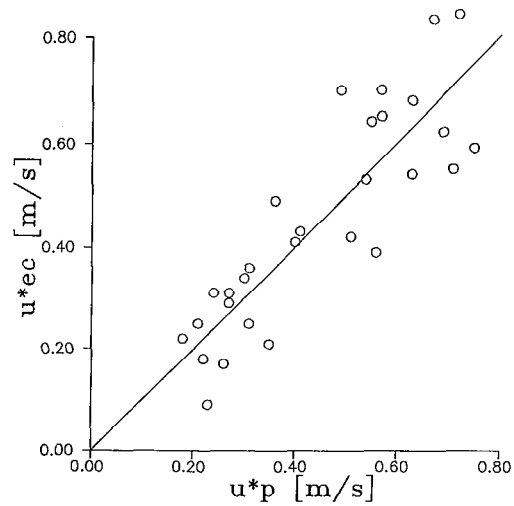

Figure 6. Comparison between the u_{*p} values obtained from the 100-m wind speed by means of the unstable drag coefficient Cd_{100} versus the u_{*ec} values. The coefficient of determination is $R^2 = 0.75$.*

Acknowledgments. We gratefully acknowledge the assistance of Ben Faber (UC Farm Advisor) for initiating the project and helping us establish and carry out the field experiment. We are most appreciative of our colleague Rick Snyder, who played a leadership role in carrying out the field experiments. In addition, we thank Changan Zhang and Steve Grattan, who helped with the eddy correlation and boundary layer measurements. Roger Shaw, K. T. Paw U, and Bob Flocchini were most generous in their loan of the eddy correlation equipment and tethersonde system. Partial support for this project came from the INCOR cooperative grant, the National Science Foundation, and the California Water Resources Center.

References

André, J. C., J.-P. Goutorbe, and A. Perrier, HAPEX-MOBILHY: A hydrologic atmospheric experiment for the study of water budget and evaporation flux at the climatic scale, *Bull. Am. Meteorol. Soc.*, *67*, 138–144, 1986.

André, J. C., et al., Evaporation over land-surfaces: First results from HAPEX—MOBILHY special Observing period, *Geophys. J. Oxford*, *6*, 477–492, 1988.

Belchov, R., and A. M. Yaglom, Comments on the theory of similarity as applied to turbulence in an unstably stratified fluid (in Russian), *Izv. Akad. Nauk. SSSR Fiz. Atmos. Okeana*, *7*, 1270–1279, 1971. (English translation, *Izv. Acad. Sci. USSR Atmos. Oceanic Phys.*, *7*, 829–934, 1971.)

Brutsaert, W., *Evaporation Into the Atmosphere: Theory, History, and Applications*, Kluwer Academic, Norwell, Mass., 1982.

Brutsaert, W., Catchment scale evaporation and the atmospheric boundary layer, *Water Resour. Res.*, *22*, 39S–45S, 1986.

Brutsaert, W., Stability correction functions for the mean wind speed and temperature in the unstable surface layer, *Geophys. Res. Lett.*, *19*, 469–472, 1992.

Brutsaert, W., and W. P. Kustas, Surface water vapor and momen-

tum fluxes under unstable conditions from a rugged-complex area, *J. Atmos. Sci.*, *44*, 421–431, 1987.

Brutsaert, W., and M. B. Parlange, The unstable surface layer above forest: Regional evaporation and heat flux, *Water Resour. Res.*, *28*, 3129–3134, 1992.

Brutsaert, W., and M. Sugita, The extent of the unstable Monin-Obukhov layer for temperature and humidity above complex hilly grassland, *Boundary Layer Meteorol.*, *51*, 383–400, 1990.

Brutsaert, W., M. B. Parlange, and J. H. C. Gash, Neutral humidity profiles in the boundary layer and regional evaporation from sparse pine forest, *Geophys. J. Oxford*, *7*, 623–630, 1989.

Businger, J., A note on the Businger-Dyer profiles, *Boundary Layer Meteorol.*, *42*, 145–151, 1988.

Cellier, P., On the validity of flux-gradient relationships above very rough surfaces, *Boundary Layer Meteorol.*, *36*, 417–419, 1986.

Chen, F., and P. Schwerdtfeger, Flux-gradient relationships for momentum and heat over a rough natural surface, *Q. J. R. Meteorol. Soc.*, *115*, 335–352, 1989.

Denmead, O. T., and E. F. Bradley, Flux gradient relationships in a forest canopy, in *The Forest-Atmosphere Interaction*, edited by B. A. Hutchinson and B. B. Hicks, pp. 421–442, D. Reidel, Norwell, Mass., 1985.

Dyer, A. J., A review of flux-profile relationships, *Boundary Layer Meteorol.*, *7*, 363–372, 1974.

Garratt, J. R., Flux profile relations above tall vegetation, *Q. J. R. Meteorol. Soc.*, *104*, 199–211, 1978.

Garratt, J. R., Comments on the paper "Analysis of the flux-profile relationships above tall vegetation—An alternative view," II, *Q. J. R. Meteorol. Soc.*, *105*, 1079–1082, 1979.

Garratt, J. R., Surface influence upon vertical profiles in the atmospheric near-surface layer, *Q. J. R. Meteorol. Soc.*, *106*, 803–819, 1980.

Gash, J. H. C., W. J. Shuttleworth, C. R. Lloyd, J. C. André, J. P. Goutorbe, and J. Gelpe, Micrometeorological measurements in Les Landes Forest during HAPEX-M|OBILHY, *Agric. For. Meteorol.*, *46*, 131–147, 1989.

Hicks, B. B., Wind profile relationships from the "Wangara" experiment, *Q. J. R. Meteorol. Soc.*, *102*, 535–551, 1976.

Hogstrom, U., Non-dimensional wind and temperature profiles in the atmospheric surface layer: A re-evaluation, *Boundary Layer Meteorol.*, *42*, 55–78, 1988.

Holtslag, A. A. M., Estimates of diabatic wind speed profiles from near surface weather observations, *Boundary Layer Meteorol.*, *29*, 225–250, 1984.

Kader, B. A., and A. M. Yaglom, Mean fields and fluctuation moments in unstably stratified turbulent boundary layers, *J. Fluid Mech.*, *212*, 637–662, 1990.

Katul, G. G., and M. B. Parlange, A Penman-Brutsaert model for wet surface evaporation, *Water Resour. Res.*, *28*, 121–126, 1992a.

Katul, G. G., and M. B. Parlange, Estimation of bare soil evaporation using skin temperature measurements, *J. Hydrol.*, *132*, 91–106, 1992b.

Kustas, W. P., and W. Brutsaert, Wind profile constants in a neutral atmospheric boundary layer over complex terrain, *Boundary Layer Meteorol.*, *34*, 35–54, 1986.

LeClerc, M. Y., and G. W. Thurtell, Footprint prediction of scalar fluxes using a Markovian analysis, *Boundary Layer Meteorol.*, *52*, 247–258, 1990.

Monin, A. S., and A. M. Obukhov, Basic laws of turbulent mixing in the ground layer of the atmosphere (in Russian), *Izv. Akad. Nauk SSSR Ser. Fiz.*, *24*(151), 163–187, 1954.

Paeschke, W., Experimentelle Untersuchungen zum Rauhigkeits- und Stabilitaetproblem in der Bodennahen Luftschicht, *Contrib. Atmos. Phys.*, *24*, 163–169, 1937.

Panofsky, H. A., and J. A. Dutton, *Atmospheric Turbulence, Models and Methods for Engineering Applications*, Wiley-Interscience, New York, 1984.

Parlange, M. B., and W. Brutsaert, Regional roughness of the Landes Forest and surface shear stress under neutral conditions, *Boundary Layer Meteorol.*, *48*, 69–81, 1989.

Parlange, M. B., and W. Brutsaert, Are radiosonde time scales appropriate to characterize boundary layer wind profiles?, *J. Appl. Meteorol.*, *29*, 249–255, 1990.

Parlange, M. B., and W. Brutsaert, Regional shear stress of broken forest from radiosonde wind profiles in the unstable surface layer, *Boundary Layer Meteorol.*, *64*, 355–368, 1993.

Parlange, M. B., and G. G. Katul, An advection-aridity evaporation model, *Water Resour. Res.*, *28*, 127–132, 1992a.

Parlange, M. B., and G. G. Katul, Estimation of the diurnal variation of potential evaporation from a wet bare soil surface, *J. Hydrol.*, *132*, 91–106, 1992b.

Paulson, C. A., The mathematical representation of wind speed and temperature profiles in the unstable atmospheric surface layer, *J. Appl. Meteorol.*, *9*, 857–861, 1990.

Raupach, M. R., Anomalies in flux-gradient relationships over forest, *Boundary Layer Meteorol.*, *16*, 467–486, 1979.

Raupach, M. R., and A. S. Thom, Turbulence in and above plant canopies, *Annu. Rev. Fluid Mech.*, *13*, 97–129, 1981.

Schuepp, P. H., M. Y. LeClerc, J. I. Macpherson, and R. L. Desjardins, Footprint prediction of scalar fluxes from analytical solutions of the diffusion equation, *Boundary Layer Meteorol.*, *50*, 355–373, 1990.

Shuttleworth, W. J., J. H. C. Gash, C. R. Lloyd, C. J. Moore, and J. S. Wallace, An integrated micrometeorogical system for evaporation measurement, *Agric. For. Meteorol.*, *43*, 295–317, 1988.

Stull, R. B., *An Introduction to Boundary Layer Meteorology*, Kluwer Academic, Norwell, Mass., 1988.

Sugita, M., and W. Brutsaert, Wind velocity measurements in the neutral boundary layer above hilly prairie, *J. Geophys. Res.*, *95*, 7617–7624, 1990.

Thom, A. S., J. B. Stewart, H. R. Oliver, and J. H. C. Gash, Comparison of aerodynamic and energy budget estimates of fluxes over pine forest, *Q. J. R. Meteorol. Soc.*, *101*, 93–105, 1975.

Zilitinkevich, S. S., Turbulence and diffusion in free convection (in Russian), *Izv. Akad. Nauk. SSSR Fiz., Atmos. Okeana*, *7*, 1263–1269, 1971. (English translation, *Izv. Acad. Sci. USSR Atmos. Oceanic Phys.*, *7*, 825–828, 1971.)

G. G. Katul, Hydrologic Science, University of California, Davis, CA 95616-8628.

M. B. Parlange, Hydrologic Science and Department of Biological and Agricultural Engineering, Veihmeyer Hall, University of California, Davis, CA 95616-8628.

(Received January 24, 1994; revised July 12, 1994;
accepted July 27, 1994.)